Mesoporous Materials

DOI: 10.1002/ange.201300326

Large Increase in the Second-Order Nonlinear Optical Activity of a Hemicyanine-Incorporating Zeolite Film**

*Tung Cao Thanh Pham, Hyun Sung Kim, and Kyung Byung Yoon**

A second-order nonlinear optical (2NLO) material generates a second harmonic (2ω) from an incident laser beam with the frequency of ω and shows electro-optic properties. 2NLO materials are currently widely used as key materials for optical communication, optical switching, laser components, IR detectors for medical and military applications, and so on. Although some 2NLO materials are commercially available, their tensor components of the quadratic NLO susceptibilities (d_{mn}) are not high enough to be used in miniature integrated photonic devices. Therefore, the search for 2NLO materials with exceptionally high activities has to be continued not only to enhance their functions in current applications but also to help expedite the materialization of photonics in which photons instead of electrons are used for signal processing, transmission, and storage.

The general approach has been to organize the molecules with large second-order hyperpolarizability (β) values into 2NLO materials.[1–29] The first methodology has been non-centrosymmetric crystallization of 2NLO molecules.[1,2] However, this methodology has been of limited success. The second methodology has been orientation-controlled layer-by-layer deposition of 2NLO molecules on substrates.[3–9] However, the procedures are highly time-consuming, and the obtained materials bear no practical applicability arising from their poor mechanical and thermal stabilities. The third methodology has been random incorporation of dipolar molecules into polymer matrices followed by subsequent electric field-assisted forced alignment of the molecules into a uniform direction, a process often called poling.[10–14] This methodology can also be named as a host–guest composite formation methodology, where a polymer is serving as a flexible organic host. However, the gradual orientation relaxation of the 2NLO molecules into the original random orientations under the application conditions or often called depoling has been a serious problem.

To overcome such problems associated with depoling, orientation-controlled insertion of 2NLO molecules into rigid inorganic hosts has received great attention. Thus Stucky,[15,16] Marlow,[17,18] Caro,[17–19] and Qiu,[20] and others started testing zeolites as the rigid hosts. The tested zeolites were $AlPO_4$-5,[15–17,19] silicalite-1,[18,20] ZSM-5,[18,19] and others.[21,22] The studied 2NLO molecules were *para*-nitroaniline and the related molecules.[17–21] Through these works, the potential of zeolites as versatile rigid inorganic hosts for preparation of practically viable inorganic–organic host–guest second-harmonic generating materials was demonstrated. However, the employed zeolite hosts were limited to powders and small single crystals that bear limited practical applicability. Furthermore, the β values of the tested 2NLO molecules were low (about 35×10^{-30} esu at 1064 nm).[23,24] Therefore, to develop commercially viable zeolite–molecule host–guest 2NLO materials, methods to grow transparent zeolite films on supports with the channels uniformly aligned and methods to incorporate 2NLO molecules with high β values into zeolite channels in uniform orientations have to be developed.

By choosing silicalite-1 (denoted as SL-1, Figure 1a) as a prototypical zeolite and hemicyanine (HC) ($\beta=760\times10^{-30}$ esu at 1064 nm) as a prototypical 2NLO molecule, our group has conducted a series of research aiming at the development of methods to prepare transparent silicalite-1 films on glass with the straight channels (5.3×5.6 Å) or b-axis oriented normal to the glass substrate and to include HC molecules into silicalite-1 channels in uniform orientations.[25–29] The structures of the mostly studied HC molecules are the HCs with different alkyl chain lengths n (HC-n, where $n=3$, 6, 9, 12, 15, 18, 22, and 24, see Figure 1b).

The two most important factors that sensitively affect the performance of HC-n-including SL-1 films are the number of included HC-n molecules per channel (N_C) per unit length (1 μm) or number density (ND) and the degree of uniform orientation (DUO) of the HC-n molecules within the channel. In the case of HC-n, they tend to enter silicalite-1 channels with the alkyl tail first as n increases (Figure 1c) and DUO tends to increase as n increases.[25] Unfortunately, however, ND decreases sharply as n increases,[25] and this has been a serious problem.

The silicalite-1 films have been grown on both sides of glass plates, which are denoted as SL_2/G. An illustration of a HC-n-incorporating SL_2/G plate is shown in Figure 1d. The thicknesses of the SL-1 films have been less than 3 μm. The 2ω intensities ($I_{2\omega}$) of the HC-n-incorporating SL_2/G plates have been measured by the Maker fringe method and the measured $I_{2\omega}$ values were compared with respect to that of a reference material (a 3 mm thick y-cut quartz crystal,

[*] Dr. T. C. T. Pham, Prof. Dr. H. S. Kim, Prof. Dr. K. B. Yoon
Korea Center for Artificial Photosynthesis
Center for Microcrystal Assembly, Department of Chemistry
Sogang University, Seoul 121-742 (Korea)
E-mail: yoonkb@sogang.ac.kr

[**] This work was supported by the Korea Center for Artificial Photosynthesis funded by the Ministry of Education of Science and Technology through the National Research Foundation of Korea, grant numbers 2012M1A2A2671784 and 2012R1A2A3A01009806. We thank J. Y. Lee for providing Figure 1 and the picture for the table of contents. We also thank KBSI Daegu for the measurements of ^{29}Si NMR spectra.

Supporting information for this article is available on the WWW under http://dx.doi.org/10.1002/anie.201300326.

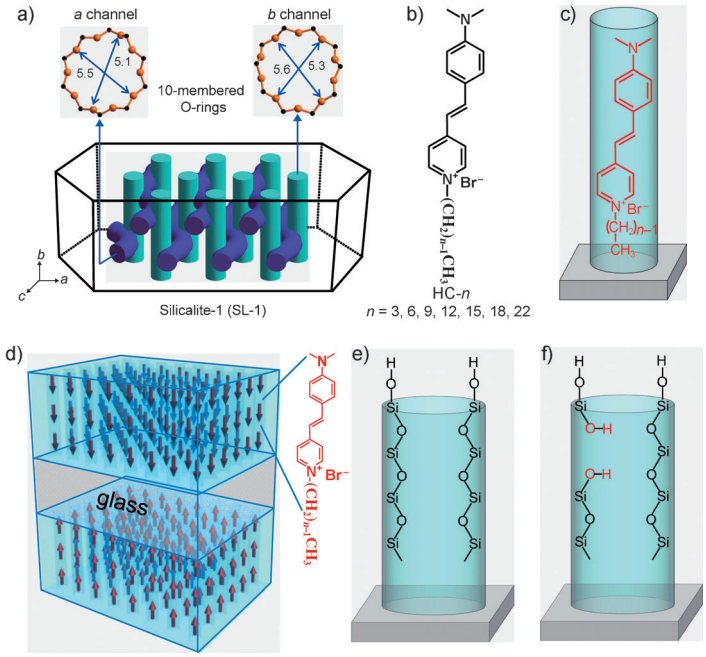

Figure 1. a) Typical crystal morphology, channel networking, and pore sizes of silicalite-1, b) structures of hemicyanine with different alkyl chain lengths (HC-*n*), c) a straight silicalite-1 channel incorporating a HC-*n* molecule with the alkyl group pointing to the substrate, d) a glass plate coated with HC-*n*-incorporating silicalite-1 films on both sides, e) an ideal defect-free silicalite-1 channel, and f) a normal silicalite-1 channel with Si atom deficiencies.

a piece of 3 mm thick quartz plate, the plane of which is perpendicular to its crystalline *y*-axis). Thus, the relative $I_{2\omega}$ (rel-$I_{2\omega}$ in %) values have been obtained for HC-*n*-incorporating SL_2/G plates and their values have been compared.

The highest rel-$I_{2\omega}$ value that has been achieved so far is 175 %.[28] This was achieved from 3 μm thick SL_2/G plates using HC-15 as the 2NLO molecule. The measured *ND* was 24 and the d_{33} value (a polarizability tensor component) was 2.7 pm V^{-1}.[28] In fact, the expected rel-$I_{2\omega}$, *ND*, and d_{33} values from an ideal 3 μm thick SL_2/G plate which is fully loaded with HC-15 with $DUO = 1$ are 1.4×10^8 %, 322, 297 pm V^{-1}, respectively. These extremely high values indicate that there are many possibilities to improve *ND*, *DUO*, and eventually d_{33} values. The first step is to develop methods to increase *ND* for HC-*n* molecules with long alkyl chains ($n \geq 15$).

Understanding of the channel structures of SL-1 is essential. An ideal channel structure is depicted in Figure 1e. However, it has been demonstrated that SL-1 contains many defects when produced from a basic gel-containing structure-directing agent.[30–32] The most common defect is the Si absence, giving rise to creation of internal hydroxyl groups (Figure 1f). The channels become hydrophilic, thereby blocking the passage of HC-*n* molecules with long hydrophobic alkyl chains.

The addition of fluoride (F^-)-liberating agents into the gel leads to a decrease of the pH value of the gel, giving rise to minimization of the number of defect sites.[31,32] Motivated by this, we have conducted a series of experiments to study the effect of F^- ions in the gel on *ND*, rel-$I_{2\omega}$, and d_{33} using ammonium hexafluoro silicate $(NH_4)_2SiF_6$ as the F^- source. We thus prepared a series of gels consisting of tetraethylorthosilicate (TEOS), tetraethyl ammonium hydroxide (TEAOH), $(NH_4)_2SiF_6$, and water at a mole ratio of TEOS:TEAOH:$(NH_4)_2SiF_6$:H_2O = 4.00:1.92:*x*:50, where $x = 0.36$, 0.54, and 0.72. Since each $(NH_4)_2SiF_6$ liberates six F^- ions, the *x* values correspond to 2.16, 3.24, and 4.32, respectively, in terms of the mole ratio of F^-. Because they are about 100, 150, and 200 % of that of TEAOH, we denote the gels as Gel-1F, Gel-1.5F, and Gel-2.0F, respectively. We also prepared a F^--free gel consisting of TEOS, tetrapropyl ammonium hydroxide (TPAOH), and water at a mole ratio of TEOS:TPAOH:H_2O = 0.8:0.1:50. This gel is denoted as Gel-0F.

We first prepared SL-1 crystals from Gel-0F, Gel-1F, Gel-1.5F, and Gel-2F. The crystals are denoted as SL-*x*F, where $x = 0$, 1, 1.5, and 2, respectively. Their magic angle spinning (MAS) ^{29}Si-NMR spectra are compared in Figure 2a. Consistent with literature reports,[31,32] SL-0F crystals showed a broad peak arising from internal Q^3 Si atoms bearing OH groups in the region between $\delta = -100$ and -105 ppm in addition to two envelopes of broad unresolved peaks arising from Q^4 Si atoms in the region between $\delta = -108$ and -118 ppm. In contrast, SL-1F, SL-1.5F, and SL-2F crystals did not show the Q^3 Si peaks, but showed ^{29}Si NMR spectra which are the same with that reported by Thomas and Fyfe.[33] This confirms that they have much less defect sites arising from the Si deficiency. Although the ^{29}Si NMR spectra

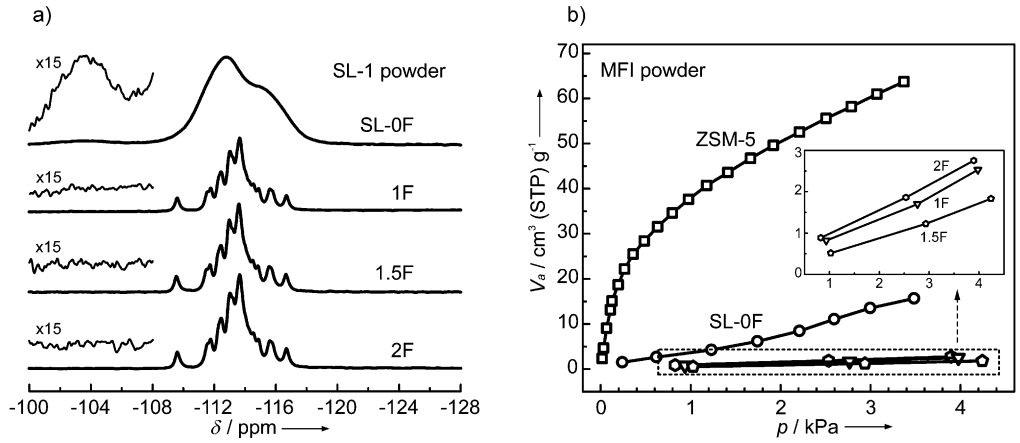

Figure 2. a) Magic angle spinning ^{29}Si NMR spectra of SL-*x*F crystals with $x = 0$, 1, 1.5, and 2 and b) water adsorption isotherms of ZSM-5 and SL-*x*F crystals.

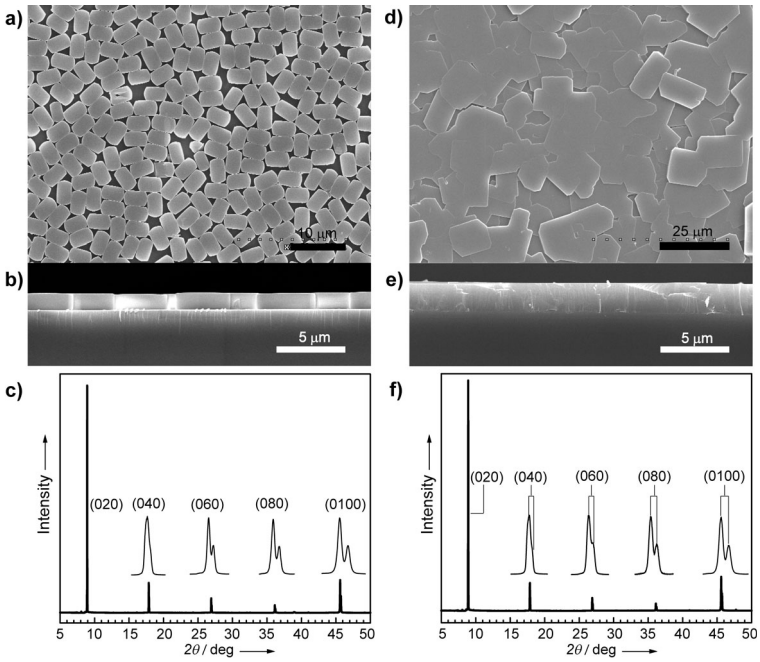

Figure 3. SEM images (a: top view, b: side view) and c) the X-ray diffraction pattern of a monolayer of silicalite-1 crystals assembled on a glass plate. SEM images (d: top view, e: side view) and f) the x-ray diffraction pattern of a continuous b-oriented silicalite-1 film grown on a glass plate using the silicalite-1 monolayers as the seed monolayers. The splitting of the diffraction peaks is due to the presence of two different wavelengths in the X-ray source (Cu $K\alpha_1$ and $K\alpha_2$).

of SL-1F, SL-1.5F, and SL-2F crystals look the same, their water adsorption isotherms (Figure 2b) showed that the hydrophobicity increases in the order: SL-0F $\ll$ SL-2F $<$ SL-1F $<$ SL-1.5F.

We also prepared monolayers of SL-1 seed crystals ($2.8 \times 1.3 \times 4.8\ \mu m^3$) on both sides of each glass plate. The typical scanning electron microscope (SEM) images of the top and side views are shown in Figure 3a,b, respectively. The X-ray diffraction pattern (Figure 3c) shows the appearance of only (0k0) peaks, again confirming that all SL-1 crystals are oriented with the *b*-axis normal to the substrate surface. The monolayer-assembled glass plates were immersed into Gel-1F, Gel-1.5F, and Gel-2F, respectively, and the corresponding SL_2/G plates were produced. The thicknesses of the SL-1 films were adjusted to be 2.4 μm. Some SL_2/G plates were also prepared from Gel-0F (see Section SI-1 in the Supporting Information for experimental details). In this case the maximum thickness that can be achieved with reasonably uniform *b*-orientation is 0.4 μm (see Section SI-2 for SEM images). Beyond this, a severe orientation randomization takes place. The obtained SL_2/G plates are denoted as SL(xF)$_2$/G, where $x = 0$, 1, 1.5 and 2. The SEM images (top and side views) of a SL(1.5F)$_2$/G are shown in Figure 3d,e. The X-ray diffraction pattern (Figure 3f) shows only (0k0) peaks, confirming that the SL-1 films are oriented with the *b*-axis normal to the substrate surface (see Section SI-1 for the conditions for XRD diffraction measurements). The full-width-at-half-maximum (fwhm) value of the (040) peak was 0.0782, which is essentially the same as that of the monolayer (0.0785), indicating the high crystallinity of the SL(1.5F) film. Likewise, SL(1F)$_2$/G and SL(2F)$_2$/G plates are all perfectly *b*-oriented and their cyrstallinities were very high.

The incorporation of HC-n into SL(xF)$_2$/G was carried out by immersing calcined SL(xF)$_2$/G plates into each methanol solution of HC-n ($n \geq 12$) for one week at room temperature. The *ND* values of HC-15 into SL(xF)$_2$/G were 23, 35, 29, and 23 for $x = 2$, 26, 30, 24, and 24 for $x = 1.5$, 18, 21, 17, and 16 for $x = 1$, 21, 14, 9, and 2 for $x = 0$, for $n = 12$, 15, 18, and 22, respectively (Supporting Information, see Section SI-3 for details). Thus, when $x \geq 1$, the *ND* value increased upon increasing n from 12 to 15 and then gradually decreased upon further increasing to 22 (Figure 4a). This mode is different from the case where $x = 0$, in which the *ND* value monotonously decreased upon increasing n from 12 to 22. In fact, the *ND* values for SL(0F)$_2$/G are obtained by simply multiplying the values obtained from a 0.4 μm thick film by 2.5. However, N_C does not linearly increase by simply increasing the thickness of the film. Therefore, the actual *ND* values for SL(0F)$_2$/G are lower than the simply estimated values. In any case, for $n = 15$, 18, and 22, the *ND* value increases with increasing x. This indicates that the number of defect site because of the Si atom deficiency progressively decreases with increasing x.

The measured rel-$I_{2\omega}$ values are plotted in Figure 4b. When $x \geq 1$ they are higher than 100%, indicating that the $I_{2\omega}$ values of the 2.4 μm thick HC-n-incorporating SL-1 films are higher than that of the 3 mm thick quartz plate. The maximum rel-$I_{2\omega}$ value was obtained from SL(1.5F)$_2$/G and HC-15, which is 400%. This is higher than the values ever observed from HC-n-incorporating thin SL-1 films (Figure 4c). The corresponding values obtained from the 2.4 μm thick SL(1F)$_2$/G and SL(2F)$_2$/G were 145 and 290%, respectively.

Interestingly, when SL(1.5F)$_2$/G plates were kept in the HC-15 solution for 1 year the *ND* value increased to 100 (see Section SI-4 for details), which corresponds to 31% of the theoretical maximum (322). The highest *ND* value observed in the past was less than 7%[28] and thus, the fact that *ND* value can reach 31% of the theoretical maximum is highly encouraging. In this case, the measured rel-$I_{2\omega}$ value was 778%, which is the highest value ever observed (Figure 4c). Note that the *ND* and rel-$I_{2\omega}$ values of the one week immersed SL(1.5F)$_2$/G were 30 and 400%, respectively. From the fact that $I_{2\omega}$ is proportional to $(N_C)^2$, the expected rel-$I_{2\omega}$ value of one-year immersed SL(1.5F)$_2$/G plate is 11 times higher than that (400%) of one-week immersed SL(1.5F)$_2$/G plate under the condition that *DUO* remains constant irrespective of *ND*. In this respect, the fact that the rel-$I_{2\omega}$ value increased by only 95% while *ND* increased by 330% indicates that *DUO* of HC-15 decreases sharply as *ND* increases.

The calculated *DUO* and d_{33} values of HC-15-incorporating SL(xF)$_2$/G are plotted in Figure 4d with respect to x. The

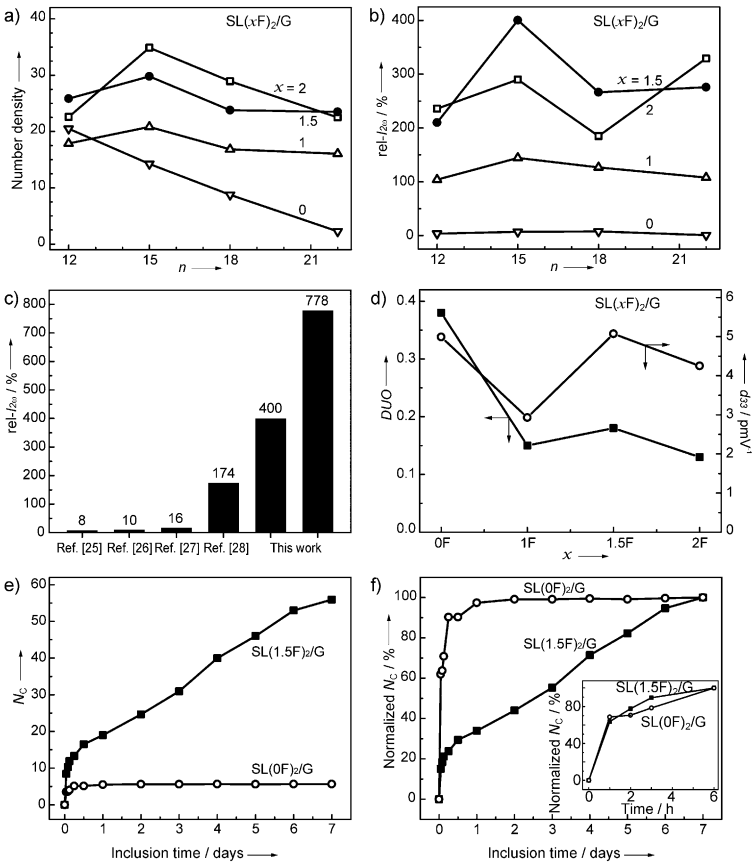

Figure 4. a) Plots of the number density (*ND*) of HC-*n* molecules with respect to *n* for each SL(*x*F)$_2$/G and b) rel-$I_{2\omega}$ of HC-*n*-incorporating SL(*x*F)$_2$/G with respect to *n* for each SL(*x*F)$_2$/G. c) Comparison of the maximum rel-$I_{2\omega}$ values obtained in this work with those in the literature. d) Plots of DUO and d_{33}, respectively, with respect to *x* in SL(*x*F)$_2$/G. e) Plots of N_c with respect to the inclusion time for SL(1.5F)$_2$/G and SL(0F)$_2$/G (N_c = number of HC-*n* dyes in each channel). f) Plots of normalized N_C (N_C with respect to maximum N_C in %) with respect to the inclusion time for SL(1.5F)$_2$/G and SL(0F)$_2$/G. The inset of (f) shows the corresponding plots of normalized N_C with respect to the inclusion time for the initial 6 h period.

DUO values of HC-15 are 0.15, 0.18, and 0.13 for $x = 1$, 1.5, and 2, respectively, which are lower than that of HC-15 for $x = 0$ (0.38). This also shows the phenomenon that *DUO* decreases as *ND* increases under our experimental condition. The highest d_{33} value was 5.1 pm V^{-1}, which is higher than those of commercially available 2NLO materials such as $LiNbO_3$ (2.76 pm V^{-1})[34] and beta-Ba_2BO_4 (BBO, $d_{22} = 2.22$, $d_{31} = 0.16$ pm V^{-1}),[34] indicating that HC-15-incorporating SL(1.5F)$_2$/G films can be commercialized by increasing the thickness. Furthermore, the measured hardness and elastic modulus values of SL(1.5F)$_2$/G were 5.99 and 51.8 GPa, respectively (see Section SI-1 for experimental details), which are much higher than those of a polymethylmethacrylate (PMMA) film, a commonly used polymer host for 2NLO dyes, (0.29 and 6.3 GPa, respectively). This result further supports the feasibility of commercialization of SL(1.5F)$_2$/G films.

We also measured the N_C values of HC-15 into SL(0F)$_2$/G and SL(1.5F)$_2$/G after various periods of inclusion (see Section SI-5 for details), and plotted the values with respect to the inclusion time (Figure 4e). In the case of SL(1.5F)$_2$/G, 30% of HC-15 (13.3 molecules) entered the channels within the initial period of 6 h and the remaining 70% (42.6 molecules) entered the channels during 162 h (6.75 d). This indicates that the inclusion of HC-15 molecules into SL(1.5F)$_2$/G undergoes in two modes, initial very rapid mode which takes care of 30% inclusion (13.3 molecules) and the subsequent slower mode which takes care of 70% inclusion (42.6 molecules). In contrast, in the case of SL(0F)$_2$/G, 90% of HC-15 (5.1 molecules) entered the channels of SL(0F)$_2$/G within the initial 6 h whereas the remaining 10% (0.55 molecules) entered the channels within 162 h, indicating that there exists only the initial rapid incorporation mode. The plots of normalized N_C values (% of N_C with respect to the maximum N_C) with respect to the inclusion time (Figure 4f) more clearly show the two different inclusion profiles of HC-15 into SL(0F)$_2$/G and SL(1.5F)$_2$/G.

Thus, SL(0F)$_2$/G has only the initial rapid incorporation mode whereas SL(1.5F)$_2$/G has two modes, the initial rapid one and the slower second one. The plots of normalized N_C values with respect to the inclusion time for the initial 6 h period (Figure 4f, inset) further show that the two initial incorporation modes are nearly the same, very rapid about 70% incorporation during the initial 1 h period and slower incorporation of the remaining 30% within the next 5 h period. The occurrence of the second slower mode in the case of SL(1.5F)$_2$/G is attributed to the slower inward diffusion of initially incorporated HC-15 molecules. The two contrasting HC-15 inclusion profiles and the fact that the initially included number of HC-15 is higher for SL(1.5F)$_2$/G (13.3) than for SL(0F)$_2$/G (5.1) also indicate that the channels of SL(0F)$_2$/G have much higher numbers of Si atom deficiency defect (Figure 1f) than those of SL(1.5F)$_2$/G. In particular, the absence of a second mode of HC-15 incorporation into the channels of SL(0F)$_2$/G indicates that the inward diffusion of HC-15 is practically prohibited by the severe internal defects.

In summary, the two most important issues towards commercialization of HC-*n*-incorporating SL-1 films for practical applications have been to increase the number density (*ND*) of HC-*n* molecules with long alkyl chains and to increase the degree of uniform orientation (*DUO*) of the HC-*n* molecules ($n \geq 15$) at the time of incorporation into SL-1. Herein, we have addressed the first issue and as a result found that the secondary growth of SL-1 films in a fluoride (F^-)-incorporating gel gives rise to a significant increase in *ND*, because of the decrease of the Si atom deficiency defects. A 2.3–4.5-fold increase in rel-$I_{2\omega}$ was achieved. The next target is to develop the methods to significantly increase *DUO*, which is still low (< 0.2). Thus, coupled with the relatively high d_{33} value (5.1 pm V^{-1}) and the phenomenon that the hardness and elastic modulus values of SL(1.5F)$_2$/G are much higher than those of a polymethylmethacrylate (PMMA) film,

a commonly used polymer host for 2NLO dyes, we demonstrate the great potential of HC-*n*-incorporating SL-1 films to replace polymer-based 2NLO materials.

Received: January 14, 2013
Published online: April 18, 2013

Keywords: channels · defect sites · dyes · nonlinear optics · zeolites

[1] C. Wang, T. Zhang, W. Lin, *Chem. Rev.* **2012**, *112*, 1084 – 1104.
[2] O. R. Evans, W. Lin, *Acc. Chem. Res.* **2002**, *35*, 511 – 522.
[3] H. E. Katz, G. Scheller, T. M. Putvinski, M. L. Schilling, W. L. Wilson, C. E. D. Chidsey, *Science* **1991**, *254*, 1485 – 1487.
[4] G. J. Ashwell, R. C. Hargreaves, C. E. Baldwin, G. S. Bahra, C. R. Brown, *Nature* **1992**, *357*, 393 – 395.
[5] D. R. Kanis, M. A. Ratner, T. J. Marks, *Chem. Rev.* **1994**, *94*, 195 – 242.
[6] X. Yang, D. McBranch, B. Swanson, D. Li, *Angew. Chem.* **1996**, *108*, 572 – 575; *Angew. Chem. Int. Ed. Engl.* **1996**, *35*, 538 – 540.
[7] G. Wang, P. Zhu, T. J. Marks, J. B. Ketterson, *Appl. Phys. Lett.* **2002**, *81*, 2169 – 2171.
[8] Y. Wang, C. Wang, X. Wang, Y. Guo, B. Xie, Z. Cui, L. Liu, L. Xu, D. Zhang, B. Yang, *Chem. Mater.* **2005**, *17*, 1265 – 1268.
[9] L. Boubekeur-Lecaque, B. J. Coe, K. Clays, S. Foerier, T. Verbiest, I. Asselberghs, *J. Am. Chem. Soc.* **2008**, *130*, 3286 – 3287.
[10] S. R. Marder, B. Kippelen, A. K.-Y. Jen, N. Peyghambarian, *Nature* **1997**, *388*, 845 – 851.
[11] C. Samyn, T. Verbiest, A. Persoons, *Macromol. Rapid Commun.* **2000**, *21*, 1 – 15.
[12] M. E. van der Boom, *Angew. Chem.* **2002**, *114*, 3511 – 3514; *Angew. Chem. Int. Ed.* **2002**, *41*, 3363 – 3366.
[13] H. Ma, A. K.-Y. Jen, L. R. Dalton, *Adv. Mater.* **2002**, *14*, 1339 – 1365.
[14] J. Luo, M. Haller, H. Li, T.-D. Kim, A. K.-Y. Jen, *Adv. Mater.* **2003**, *15*, 1635 – 1638.
[15] S. D. Cox, T. E. Gier, G. D. Stucky, J. Bierlein, *J. Am. Chem. Soc.* **1988**, *110*, 2986 – 2987.
[16] S. D. Cox, T. E. Gier, G. D. Stucky, *Chem. Mater.* **1990**, *2*, 609 – 619.
[17] F. Marlow, J. Caro, L. Werner, J. Kornatowski, S. Dähne, *J. Phys. Chem.* **1993**, *97*, 11286 – 11290.
[18] G. Reck, F. Marlow, J. Kornatowski, W. Hill, J. Caro, *J. Phys. Chem.* **1996**, *100*, 1698 – 1704.
[19] L. Werner, J. Caro, G. Finger, J. Kornatowski, *Zeolites* **1992**, *12*, 658 – 663.
[20] F. Gao, G. Zhu, Y. Chen, S. Qiu, *J. Phys. Chem. B* **2004**, *108*, 3426 – 3430.
[21] I. Kinski, P. Daniels, C. Deroche, B. Marler, H. Gies, *Microporous Mesoporous Mater.* **2002**, *56*, 11 – 25.
[22] J. Yu, Y. Cui, C. Wu, Y. Yang, Z. Wang, M. O'Keeffe, B. Chen, G. Qian, *Angew. Chem.* **2012**, *124*, 10694 – 10697; *Angew. Chem. Int. Ed.* **2012**, *51*, 10542 – 10545.
[23] K. Clays, A. Persoons, *Phys. Rev. Lett.* **1991**, *66*, 2980 – 2983.
[24] M. Stähelin, D. M. Burland, J. E. Rice, *Chem. Phys. Lett.* **1992**, *191*, 245 – 250.
[25] H. S. Kim, S. M. Lee, K. Ha, C. Jung, Y.-J. Lee, Y. S. Chun, D. Kim, B. K. Rhee, K. B. Yoon, *J. Am. Chem. Soc.* **2004**, *126*, 673 – 682.
[26] H. S. Kim, T. T. Pham, K. B. Yoon, *J. Am. Chem. Soc.* **2008**, *130*, 2134 – 2135.
[27] H. S. Kim, K. W. Sohn, Y. Jean, H. Min, D. Kim, K. B. Yoon, *Adv. Mater.* **2007**, *19*, 260 – 263.
[28] T. C. T. Pham, H. S. Kim, K. B. Yoon, *Science* **2011**, *334*, 1533 – 1538.
[29] H. S. Kim, T. C. T. Pham, K. B. Yoon, *Chem. Commun.* **2012**, *48*, 4659 – 4673.
[30] G. Boxhoorn, A. G. T. G. Kortbeek, G. R. Hays, N. C. M. Alma, *Zeolites* **1984**, *4*, 15 – 21.
[31] J. M. Chezeau, L. Delmotte, J. L. Guth, Z. Gabelica, *Zeolites* **1991**, *11*, 598 – 606.
[32] M. A. Camblor, L. A. Villaescusa, M. J. Díaz-Cabãnas, *Topics in Catal.* **1999**, *9*, 59 – 76.
[33] C. A. Fyfe, G. C. Gobbi, J. Klinowski, J. M. Thomas, S. Ramdas, *Nature* **1982**, *296*, 530 – 533.
[34] M. Brinkmann, J. Hayden, M. Letz, S. Reichel, C. Click, W. Mannstadt, B. Schreder, S. Wolff, S. Ritter, M. J. Davis, T. E. Bauer, H. Ren, Y.-H. Fan, S.-T. Wu, K. Bonrad, E. Krätzig, K. Buse, R. A. Paquin in *Springer Handbook of Lasers and Optics*, (Ed.: F. Träger), Springer, **2007**, pp. 309 – 311.

